Shape of a Stretched Polymer

Alberto S. Sassi, Salvatore Assenza,* and Paolo De Los Rios
Laboratoire de Biophysique Statistique, Ecole Polytechnique Fédérale de Lausanne (EPFL), CH-1015 Lausanne, Switzerland
(Received 9 June 2015; revised manuscript received 4 April 2017; published 18 July 2017)

The shape of a polymer plays an important role in its interactions with surrounding molecules. We characterize the shape and the orientational properties of a polymer chain under tension in a good solvent, a physical condition that is often realized both in single-molecule experiments and *in vivo*. Our findings reveal the existence of hitherto unobserved universal laws encompassing polymers with different rigidities and including the possible presence of excluded-volume effects, showing that both shape and orientation are solely determined by the force contribution to the free energy. In doing so, they also provide a simple way to retrieve these quantities from the knowledge of the force-versus-extension curve.

DOI: 10.1103/PhysRevLett.119.037801

Polymer chains are strongly fluctuating objects. Because of their soft nature, they do not have well-defined shapes, but rather adapt their conformational ensembles to the environment. At the same time, the shape of a polymer affects the mutual interactions with other molecules in solution, e.g., quantitatively determining the excluded volume of the chain [1,2]. In a poor solvent, polymers collapse into a roughly spherical shape, as seen, for example, in the case of single-chain globular proteins [3]. In the case of θ- or good-solvent conditions, conformations can fluctuate more wildly and the shape of a polymer is particularly sensitive to the environment. In the last two decades, many theoretical and experimental works have investigated how the shape depends on several factors such as confinement [4–8], topology [9–11], or crowding [3,12–14], which are relevant to many cellular processes.

A topic of broad interest in polymer physics is certainly the response of a polymer chain to the action of a mechanical force, a situation that is very frequent both *in vivo* and *in vitro*. For example, during replication DNA is repeatedly pulled and twisted by enzymes [15], and proteins are actively pulled by chaperones across membranes and out of ribosomes [16–22]. Moreover, the recent development of several single-molecule techniques such as atomic force microscopy and optical and magnetic tweezers has stimulated a large amount of experimental work involving polymer stretching [23]. From the theoretical point of view, the effect of an external pulling force on the shape of a polymer in a poor solvent has been previously addressed by means of Langevin simulations [24].

In this Letter, we study the deformation of a polymer under a pulling force in a good solvent. Our findings unveil the presence of a universal behavior in both the shape and orientation of stretched chains of different sizes and rigidities. These results hold regardless of the presence of excluded volume, even in the regime where the latter is strongly affecting the response of the polymer as measured by the force-versus-extension curve. In Fig. 1 we show a schematic picture recapitulating the evolution of the polymer as the tension is increased. As the picture qualitatively shows, the effect of an external force on a chain is twofold. Small forces mostly affect the overall orientation of the polymer, aligning it along their direction [25] (left region in Fig. 1). Beyond this "dipolelike" regime, the tension strongly deforms the polymer, thus leading to an increase in the anisotropy of its average shape (right region in Fig. 1).

We start our analysis by considering the simple case of a freely jointed chain (FJC). Apart from describing the behavior of virtually all kinds of polymers at extremely high forces [26], this model also enables the computation of analytical results for most of the relevant quantities. We will show later by means of numerical simulations that our results are valid also for more realistic models. The simplest quantities used to determine the conformation of a chain are the mean square of the end-to-end vector $\boldsymbol{R_e}$ and the radius of gyration R_g [1]. In the case of a FJC of N monomers with a Kuhn length b under an external force f, they can be computed straightforwardly, giving

$$\langle \boldsymbol{R_e}^2 \rangle = Nb^2(1-\mathcal{L}^2) + N^2b^2\mathcal{L}^2 \tag{1}$$

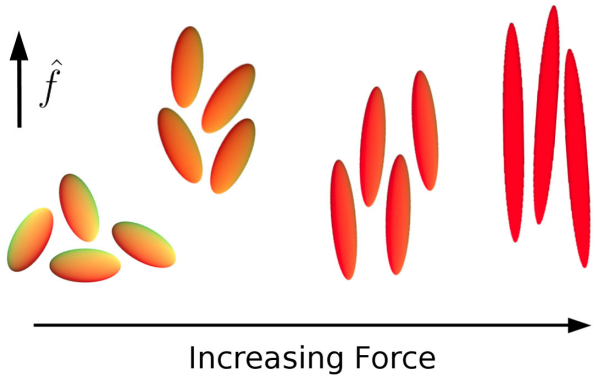

FIG. 1. Schematic illustration of the effect of an external force on a polymer in a good solvent.

and

$$\langle R_g^2 \rangle = \frac{1}{6} N b^2 + \frac{1}{12} N^2 b^2 \mathcal{L}^2, \tag{2}$$

where $\mathcal{L}(\gamma)$ is the Langevin function and $\gamma = fb/k_B T$, k_B being the Boltzmann constant and T the temperature (see Sec. S1 in the Supplemental Material [27]). As expected, we find the unperturbed results $\langle \boldsymbol{R_e}^2 \rangle \simeq N b^2$, $\langle R_g^2 \rangle \simeq N b^2/6$ when $\gamma \to 0$, and the typical values of a rod $\langle \boldsymbol{R_e}^2 \rangle \simeq N^2 b^2$, $\langle R_g^2 \rangle \simeq N^2 b^2/12$ in the limit of infinite forces. The transition between the two regimes takes place at a force $\gamma \sim 1/\sqrt{N}$, in agreement with previous perturbative results [28].

In order to capture the presence of anisotropies, we consider the inertia tensor $\mathcal{T}$, whose elements are $\mathcal{T}_{\alpha\beta} = [1/(N+1)] \sum_{i=0}^{N} (\alpha_i - \alpha_{\rm cm})(\beta_i - \beta_{\rm cm})$, where α and β are space coordinates and $(x_{\rm cm}, y_{\rm cm}, z_{\rm cm})$ is the position of the center of mass of the chain [29]. The ensemble averages of the eigenvalues of $\mathcal{T}$ of an unperturbed FJC are in the ratios $\langle \lambda_1 \rangle : \langle \lambda_2 \rangle : \langle \lambda_3 \rangle = 11.8 : 2.7 : 1$, which indicate a pronounced asymmetry in the spatial distribution of the monomers [29]. A useful global index to determine the average shape of a chain in three dimensions is provided by the asphericity [29,30]:

$$\mathcal{A} \equiv \frac{\sum_s \langle (\lambda_s - \bar{\lambda})^2 \rangle}{6 \langle \bar{\lambda}^2 \rangle} = \frac{3 \langle {\rm Tr}(\mathcal{T}^2) \rangle}{2 \langle ({\rm Tr}\mathcal{T})^2 \rangle} - \frac{1}{2}, \tag{3}$$

where $\bar{\lambda} = \sum_s \lambda_s/3 = \langle R_g^2 \rangle/3$. The asphericity of an unperturbed FJC can be computed analytically and it has been shown that, at the leading term, $\mathcal{A} = 10/19 \simeq 0.526$, independently of N [29]. We extended the computation to the case of a stretched FJC following an approach proposed by Rubinstein for the computation of $\langle R_g^2 \rangle$ in the case of an unperturbed FJC [1]. The main idea consists in rewriting the terms appearing in Eq. (3) as suitable sums of the average squared end-to-end distances of subchains of the polymer. Since for a FJC the force is applied independently to each bond, the averages can be computed by applying Eq. (1) to the subchain under consideration. The complete derivation and the full explicit formula for $\mathcal{A}$ are reported Sec. S2 of the Supplemental Material [27]. Retaining only the leading terms, the asphericity can be written as

$$\mathcal{A} = \frac{120 + 60\eta + 5\eta^2}{228 + 84\eta + 5\eta^2}, \tag{4}$$

where $\eta \equiv \boldsymbol{f} \cdot \langle \boldsymbol{R_e} \rangle / k_B T$. This formula accurately approximates the exact solution, with a maximum relative error below 1% for reasonably long chains ($N > 20$). According to Eq. (4), the asphericity of a FJC depends only on the force contribution to the free energy of the system, irrespective of the size of the chain. This universal behavior extends also to more realistic models accounting for the rigidity of the polymer or the presence of excluded-volume effects. This can be clearly seen from Fig. 2, where we report the values of

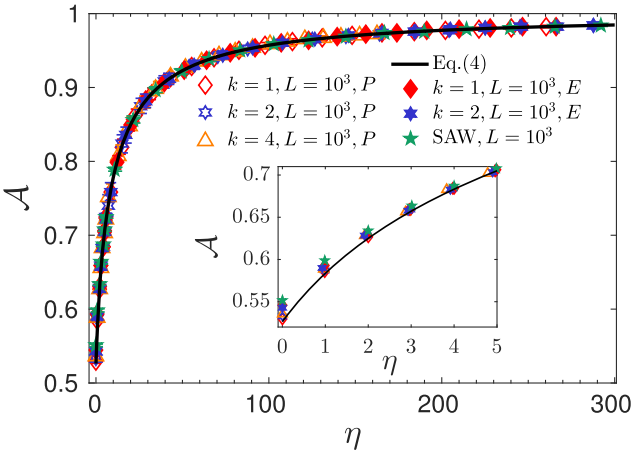

FIG. 2. Asphericity as a function of $\eta = \boldsymbol{f} \cdot \langle \boldsymbol{R_e} \rangle / k_B T$ for different models. The data correspond to WLCs of length $L = 1000$ characterized by rigidities $k = 1$ (red diamonds), $k = 2$ (blue hexagrams), and $k = 4$ (orange triangles). The green pentagrams correspond to a self-avoiding walk. Full and empty symbols respectively denote chains with (E) and without (P) excluded volume. The continuous black line represents the FJC formula reported in Eq. (4). Inset: Enlargement of the plot for small values of η.

$\mathcal{A}$ as a function of η obtained from Langevin simulations [31] of wormlike chains with several rigidities, with and without excluded volume (see Sec. S3 of the Supplemental Material for technical details [27]). The data from the simulations nicely collapse onto the same master curve identified in the FJC case [Eq. (4), continuous curve], regardless of the particular model considered. In Fig. S2 of the Supplemental Material [27] we report the corresponding force-versus-extension curves, which show that both rigidity and (when present) excluded volume significantly affect the response of the chain in the considered range of forces. Indeed, the results without excluded volume fall onto the theoretical wormlike chain (WLC) formula (dashed curve), which departs from the corresponding FJC prediction (dotted curve), thus indicating the importance of rigidity in the response of the chain. Analogously, significant effects from excluded volume are reflected in the departure of the corresponding points from the WLC formula. Nevertheless, we stress that this collapse is not exact, particularly at low forces, as we can see in the inset of Fig. 2. Finally, we note that Eq. (4) enables a direct computation of the asphericity from the knowledge of the variable η, which can be easily accessed in pulling experiments. For example, in Sec. S11 of the Supplemental Material we deduce the asphericity corresponding to force-versus-extension data obtained for dsDNA [27,32,33], which can be properly modeled by means of the WLC model [34].

We now turn our attention to the behavior of the eigenvalues and eigenvectors of the inertia tensor. In Fig. 3 (top) and Fig. S3 of the Supplemental Material [27] we report the average eigenvalues of $\mathcal{T}$ obtained from

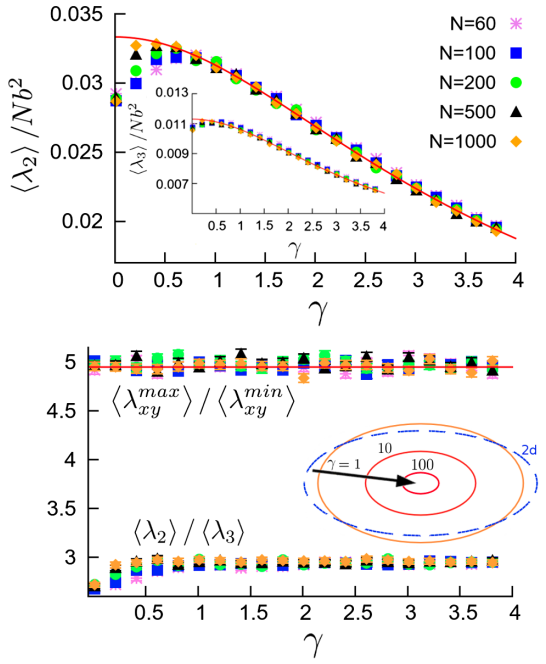

FIG. 3. Top panel: normalized eigenvalues λ_2/Nb^2 (main) and λ_3/Nb^2 (inset) as a function of γ, for several values of chain size N. The continuous curves are the corresponding fitting functions reported in the main text. Bottom panel: aspect ratio of the xy projection of the chain and of the transverse section of the ellipsoid. The continuous red line shows the aspect ratio of a pure two-dimensional FJC, which we found to be equal to 4.95 ± 0.01. Inset: sketch of the shape of the transverse section of the chain for different values of γ. The arrow indicates the direction of increasing γ. The blue dashed line sketches the typical shape of a two-dimensional FJC.

Monte Carlo (MC) simulations in the case of the FJC (see Sec. S3 of the Supplemental Material for technical details [27]). For large forces, the rodlike behavior dominates the eigenvalue response in the longitudinal direction ($\lambda_1 \propto N^2$), while the size dependence of an unperturbed chain is expected to hold for the transverse extension of the polymer ($\lambda_{2,3} \propto N$). Quantitatively, the largest eigenvalue λ_1 gives the leading contribution to Rg^2. From Eq. (2), we thus expect $\langle\lambda_1\rangle \simeq N^2b^2\mathcal{L}^2/12$, which is verified by MC simulations (Fig. S3 of Ref. [27]), with small but systematic deviations that decrease for longer chains. Analogously, the two remaining eigenvalues are expected to behave in the same way as the transverse contributions to R_g^2. We thus predict that for the large-force regime one has $\langle\lambda_2\rangle \simeq c_2Nb^2\mathcal{L}/\gamma$ and $\langle\lambda_3\rangle \simeq c_3Nb^2\mathcal{L}/\gamma$, where c_2 and c_3 are numeric constants. A simple estimation of c_2 and c_3 can be obtained by solving the eigenvalue equation for $\mathcal{T}$ with preaveraged coefficients (see Sec. S6 of Ref. [27]), and gives $c_2 \simeq (1+\sqrt{3/14})/15 \simeq 0.098$ and $c_3 \simeq (1-\sqrt{3/14})/15 \simeq 0.036$. Our ansatz is confirmed in Fig. 3 (top), where the continuous curves are obtained by tuning the coefficients in order to globally fit the MC data obtained for $\gamma > 1$ and correspond to $c_2 = 0.100 \pm 0.001$ and $c_3 = 0.034 \pm 0.001$, in good agreement with the estimated values. Intriguingly, $\langle\lambda_2\rangle$ and $\langle\lambda_3\rangle$ show a nonmonotonic behavior for small forces. A comparison with the average orientation of the corresponding eigenvectors (see Figs. S5 and S6 of Ref. [27]) shows that the range of forces with increasing λ_2, λ_3 corresponds to a regime where the ellipsoid is not aligned with the force. Therefore, an intuitive explanation of this feature is that, because of the random orientation of the polymer (see the left region in Fig. 1), on average in this regime the force deforms the ellipsoid almost isotropically, thus leading to an increase of all the eigenvalues. In contrast, after the alignment has been achieved (right region in Fig. 1), only $\langle\lambda_1\rangle$ keeps growing, while the other eigenvalues shrink due to the decreasing fluctuations in the directions perpendicular to the force.

Notably, in the large-force regime $\langle\lambda_2\rangle/\langle\lambda_3\rangle = c_2/c_3 \simeq 3$ for all values of N [Fig. 3 (bottom)]. The implication is that, once the polymer is aligned with the force, the section of the ellipsoid shrinks while preserving a uniform transverse shape that is independent of the size of the chain (inset). We note that this section does not correspond to the projection of the polymer onto the xy plane. Because of the independence of the three directions of a random walk, the projection has the same features of a two-dimensional FJC, and its shape properties are obtained by diagonalizing the submatrix of the inertia tensor identified by the elements $\mathcal{T}_{xx}, \mathcal{T}_{xy}, \mathcal{T}_{yy}$. As we report in Fig. 3 (bottom), the ratio between the averages of its eigenvalues $\lambda_{xy}^{\max}$ and $\lambda_{xy}^{\min}$ closely follows the behavior of a two-dimensional FJC (red continuous curve), but is larger than $\langle\lambda_2\rangle/\langle\lambda_3\rangle$. The reason for this discrepancy lies in the fact that the major axis of the ellipsoid gives a significant contribution to the xy projection even in the regime of large forces (see Sec. S5 of the Supplemental Material for details [27]). A similar trend is observed for the WLC model and in the presence of excluded volume. Naturally, the explicit formula for $\langle R_g^2\rangle$ depends on the particular model considered; thus, the eigenvalues show nonuniversal behaviors (see Figs. S7, S8, and S9 of Ref. [27]). However, in all the studied cases the ratio $\langle\lambda_2\rangle/\langle\lambda_3\rangle$ promptly falls onto a constant value as a function of the external force (Fig. S10 of Ref. [27]). The presence of a uniform shrinking of the transverse section of the ellipsoid encompasses all the different models considered, thus outlining a novel universal behavior in the shape of polymers. Moreover, the value of the plateau is always very close to 3, although slight differences between the different models are clearly observed, with larger deviations for stiffer polymers.

In order to study the overall orientation of a stretched polymer, we now consider the eigenvectors of $\mathcal{T}$. In Fig. 4 and in Figs. S11–S13 of Ref. [27] we show the average values of $\cos\psi_s$, where ψ_s is the angle between the applied force and the eigenvector corresponding to the eigenvalue λ_s, as a function of η. Even for this quantity, all the data

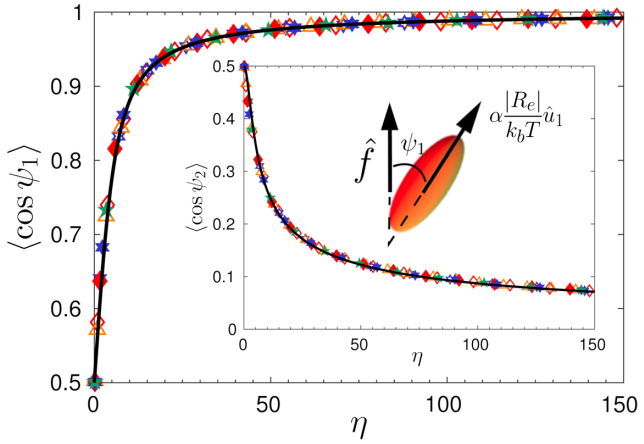

FIG. 4. Collapse of the average values of $\cos\psi_1$ (main figure) and $\cos\psi_2$ (inset) when plotted as a function of η for different models. The continuous curves are the predictions obtained from the electric-dipole analogy [Eqs. (5) and (6), respectively]. The symbols used are the same as in Fig. 2. The sketch in the inset qualitatively describes the dipole analogy.

corresponding to different sizes and models collapse onto a master curve. In this regard, we observe that the alignment of the ellipsoid to the external force is analogous to the behavior of an electric dipole in the presence of an external field [35], although here a 180° rotation results in the same physical state. Within this analogy, we can consider a dipole moment equal to $\alpha|\langle \boldsymbol{R_e} \rangle|/k_BT$, where α is a proportionality constant, and directed along the main axis of the ellipsoid, as sketched in Fig. 4. The dipole potential is $\alpha\eta\cos\psi_1$, and the average cosines are (see Sec. S9 of Ref. [27])

$$\langle \cos\psi_1 \rangle = \frac{1}{1-e^{-\alpha\eta}} - \frac{1}{\alpha\eta} \tag{5}$$

and

$$\langle \cos\psi_2 \rangle = \langle \cos\psi_3 \rangle = \frac{I_1(\alpha\eta)}{\sinh(\alpha\eta)}, \tag{6}$$

where I_1 is the modified Bessel function of the first kind. The constant α can be determined by considering the large-force behavior in the case of a FJC. Indeed, from Eq. (5), we can estimate the average sine of ψ_1 for $\gamma \gg 1$ as $\langle \sin\psi_1 \rangle \simeq \sqrt{2/(\alpha N\gamma\mathcal{L})}$. Moreover, since in this limit $\langle \lambda_1 \rangle \simeq (Nb\mathcal{L})^2$, while its xy projection is given by $c_1 Nb^2\mathcal{L}/\gamma$, we also have

$$\langle \sin\psi_1 \rangle \simeq \sqrt{\frac{c_1 Nb^2\mathcal{L}}{\gamma\langle\lambda_1\rangle}} \simeq \sqrt{\frac{12c_1}{N\gamma\mathcal{L}}}. \tag{7}$$

Comparing the two formulas for $\langle \sin\psi_1 \rangle$, we find $\alpha = 1/(6c_1) \simeq 5/6 \simeq 0.83$. Inserting this value into Eqs. (5) and (6), we obtain the continuous curves showed in Fig. 4 and Figs. S11–S13 of Ref. [27]. The remarkable agreement between our ansatz and the simulations shows that the dipole analogy can capture even quantitatively the behavior of the ellipsoid in the whole range of forces.

In conclusion, we have provided a quantitative description of the deformation of a polymer under the effect of an external force $\boldsymbol{f}$. Our findings unveil the existence of a universal response of the stretched chain, both in its shape and orientation properties. Indeed, on the one hand we have shown that at large forces the transverse section of the polymer shrinks maintaining a constant aspect ratio, which is different from the projection of the chain on the plane perpendicular to the force. On the other hand, the overall shape and orientation of the polymer (described by the asphericity and the direction of the principal eigenvector of the inertia tensor) depend on $\boldsymbol{f}$ only by means of the combination $\eta = \boldsymbol{f}\cdot\langle \boldsymbol{R_e} \rangle/k_BT$ [Eqs. (4)–(6)], representing the contribution of the force to the free energy. These results hold irrespective of the size and the rigidity of the polymer, or the possible presence of excluded-volume effects. Apart from their interest from a polymer-physics perspective, our results provide a handy tool to access the average shape and orientation of a chain in a good solvent from the mere knowledge of its force-versus-extension curve.

The authors thank the Swiss National Science Foundation for support under Grants No. 513469 (P. D. L. R. and A. S. S.) and No. 200021-138073 (P. D. L. R. and S. A.).

*salvatore.assenza@gmail.com
Present address: Laboratory of Food and Soft Materials, ETH Zürich, CH-8092 Zürich, Switzerland.

[1] M. Rubinstein and R. H. Colby, *Polymer Physics* (Oxford University Press, Oxford, 2003).
[2] A. P. Minton, Biophys. J. **78**, 101 (2000).
[3] R. I. Dima and D. Thirumalai, J. Phys. Chem. B **108**, 6564 (2004).
[4] C. E. Cordeiro, M. Molisana, and D. Thirumalai, J. Phys. II (France) **7**, 433 (1997).
[5] D. J. Bonthuis, C. Meyer, D. Stein, and C. Dekker, Phys. Rev. Lett. **101**, 108303 (2008).
[6] C. Micheletti and E. Orlandini, Macromolecules **45**, 2113 (2012).
[7] F. Benedetti, A. Japaridze, J. Dorier, D. Racko, R. Kwapich, Y. Burnier, G. Dietler, and A. Stasiak, Nucleic Acids Res. **43**, 2390 (2015).
[8] C. Haber, S. A. Ruiz, and D. Wirtz, Proc. Natl. Acad. Sci. U.S.A. **97**, 10792 (2000).
[9] G. Zifferer and W. Preusser, Macromol. Theory Simul. **10**, 397 (2001).
[10] K. Alim and E. Frey, Phys. Rev. Lett. **99**, 198102 (2007).
[11] E. J. Rawdon, J. C. Kern, M. Piatek, P. Plunkett, A. Stasiak, and K. C. Millett, Macromolecules **41**, 8281 (2008).

[12] W. K. Lim and A. R. Denton, J. Chem. Phys. **141**, 114909 (2014).
[13] M. S. Cheung, D. Klimov, and D. Thirumalai, Proc. Natl. Acad. Sci. U.S.A. **102**, 4753 (2005).
[14] D. Homouz, M. Perham, A. S. M. S. Cheung, and P. Wittung-Stafshede, Proc. Natl. Acad. Sci. U.S.A. **105**, 11754 (2008).
[15] C. Bustamante, Z. Bryant, and S. B. Smith, Nature (London) **421**, 423 (2003).
[16] K. E. Matlack, B. Misselwitz, K. Plath, and T. A. Rapoport, Cell **97**, 553 (1999).
[17] W. Neupert and M. Brunner, Nat. Rev. Mol. Cell Biol. **3**, 555 (2002).
[18] L. Liu, R. T. McNeilage, L. X. Shi, and S. M. Theg, Plant Cell **26**, 1246 (2014).
[19] B. Liu, Y. Han, and S. Qian, Mol. Cell **49**, 453 (2013).
[20] D. H. Goldman, C. M. Kaiser, A. Milin, M. Righini, I. T. Jr., and C. Bustamante, Science **348**, 457 (2015).
[21] P. De Los Rios, A. Ben-Zvi, O. Slutsky, A. Azem, and P. Goloubinoff, Proc. Natl. Acad. Sci. U.S.A. **103**, 6166 (2006).
[22] S. Assenza, P. De Los Rios, and A. Barducci, Front. Mol. Biosci. **2**, 8 (2015).
[23] F. Ritort, J. Phys. Condens. Matter **18**, R531 (2006).
[24] G. Morrison, C. Hyeon, N. M. Toan, B. Y. Ha, and D. Thirumalai, Macromolecules **40**, 7343 (2007).
[25] C. Micheletti, D. Marenduzzo, and E. Orlandini, Phys. Rep. **504**, 1 (2011).
[26] N. M. Toan and D. Thirumalai, Macromolecules **43**, 4394 (2010).
[27] See Supplemental Material at http://link.aps.org/supplemental/10.1103/PhysRevLett.119.037801 for explicit computations of the formulas, technical details on the simulations, and supplementary figures.
[28] R. M. Neumann, Biophys. J. **85**, 3418 (2003).
[29] J. Rudnick and G. Gaspari, J. Phys. A **19**, L191 (1986).
[30] J. Rudnick and G. Gaspari, *Elements of the Random Walk* (Cambridge University Press, Cambridge, England, 2004).
[31] S. Plimpton, J. Comput. Phys. **117**, 1 (1995).
[32] C. Bouchiat, M. Wang, J.-F. Allemand, T. Strick, S. Block, and V. Croquette, Biophys. J. **76**, 409 (1999).
[33] M. D. Wang, H. Yin, R. Landick, J. Gelles, and S. M. Block, Biophys. J. **72**, 1335 (1997).
[34] J. F. Marko and E. D. Siggia, Macromolecules **28**, 8759 (1995).
[35] R. M. Neumann, Phys. Rev. A **31**, 3516(R) (1985).